

# Phase space evolution of cold atoms in the presence of a weakly disordered potential

Shuyu Zhou, Julien Chabé,<sup>\*</sup> Ran Salem,<sup>†</sup> Tal David, David Groswasser, Mark Keil,<sup>‡</sup> Yonathan Japha, and Ron Folman  
*Department of Physics, Ben-Gurion University of the Negev, Be'er Sheva 84105, Israel*

(Dated: October 4, 2018)

We study the phase space evolution of cold atoms oscillating in a harmonic trap in the presence of a weak potential disorder. We demonstrate a full tomographic reconstruction of the atomic phase space distribution from a series of real-space images of the trapped atoms. For oscillation times on the order of the mean time between collisions we observe squeezing of the phase space distribution and deformations determined by the specific shape of the potential corrugations. This evolution is interpreted as angular velocity dispersion of iso-energetic trajectories in phase space. We discuss the effects of collisions and coupling between different dimensions, as well as possible applications of the method for probing classical or quantum dynamics of cold atoms.

PACS numbers: 03.65.Wj, 03.75.-b, 37.10.Gh, 67.85.-d

## INTRODUCTION

Weak disorder in otherwise smooth or perfectly periodic potentials can have significant physical effects. It is well known for example, that a disordered potential induces Anderson localization of quantum particles [1–3]. Small disorders can induce dramatic changes even in classical mechanics, for example, by coupling the separate dimensions so that the system becomes non-integrable [4]. Previous work has shown that disorder can cause a range of effects, from synchronization of coupled nonlinear oscillators under certain conditions [5] to stabilization of soliton solutions in nonlinear oscillators [6]. Very recently, theoretical work investigated the impact of weak disorder on the dynamics of classical particles in a periodically oscillating lattice [7].

Potential corrugations cause density fluctuations – and even fragmentation – as ultracold atom clouds are brought close to current-carrying wires in magnetic traps [8, 9]. This indicates that the magnetic potential produced by such wires is corrugated due to the effect of edge, surface, and bulk defects in the wire. Solid-state structures and electronic transport characteristics can be revealed by investigating these potential corrugations [10, 11]. Although such potential corrugations have been reduced significantly by static techniques, such as improved wire fabrication [12, 13], and by dynamic techniques such as using time-averaged potentials [14, 15], the residual corrugation has obvious harmful effects when highly smooth magnetic potentials are needed, for example, in guided atomic interferometers [16, 17] and free-oscillation atom interferometers [18]. The study of weakly-corrugated potentials can therefore shed light on intrinsically interesting dynamics, and is furthermore necessary for the development of technological applications.

When an atomic cloud oscillates in a trap with a pure harmonic potential, the oscillation persists indefinitely in the absence of inter-atomic collisions. Even in the presence of collisions, displacement of an atomic cloud, ini-

tially at equilibrium in a harmonic trap, does not cause any change in the phase-space distribution relative to the center of mass [19]. However, even a small potential disorder can induce damping of the oscillations [15]. A powerful approach for characterizing the dynamical evolution of such perturbed oscillations may be realized by measuring the phase space distribution of the atomic cloud [20]. To the best of our knowledge, no detailed studies have yet been done of the phase space evolution of ultracold atoms in anharmonic potentials; furthermore, real-space dynamical studies in anharmonic traps have heretofore been done at temperatures and/or densities where small nano-Kelvin disorders are not expected to play a significant role [21, 22]. Tomography provides a method to reconstruct such phase space distributions from experimental data [23], as has been demonstrated for photonic states [24] and for an atomic beam [25].

In this Letter we measure the phase space dynamics of a cold atomic cloud oscillating in a harmonic trap with small potential corrugations and we analyze these dynamics theoretically. In addition to the interesting physical aspects of phase-space evolution such as squeezing, and new insights allowing better designs for technological applications, we demonstrate that even very weak potential corrugations can significantly alter the phase space distribution, thus providing a novel and very sensitive probe of such weak corrugations.

## THEORY

As background for our analysis of the phase space dynamics, we first consider atoms moving without collisions in a trapping potential separable into a longitudinal part  $V(x)$  and a transverse part (along  $y$  and  $z$ ), such that the dynamics along  $x$  are independent of the transverse coordinates. For temperatures sufficiently in excess of the critical temperature for condensation, the evolution can be treated classically according to New-

ton's equations of motion

$$\dot{x} = p/m, \dot{p} = F(x), \quad (1)$$

where  $m$  is the mass and  $F(x) = -\partial_x V(x)$  is a position-dependent force. For a potential  $V(x)$  having a global minimum at  $x = 0$ , it is useful to define radial phase space coordinates  $r$  and  $\theta$  such that  $x = r \cos \theta$  and  $p = m\omega_0 r \sin \theta$ , with  $\omega_0$  being the harmonic frequency characterizing the potential. Equation (1) implies that the evolution follows phase space trajectories with constant energy

$$\frac{1}{2}m\omega_0^2 r^2 + \Delta U(x) = E = \text{const.}, \quad (2)$$

where  $\Delta U(x) \equiv V(x) - \frac{1}{2}m\omega_0^2 x^2$  is the deviation of the potential from a pure harmonic. For a phase space trajectory with energy  $E$  we obtain a position-dependent phase space angular velocity

$$\omega_{\text{ps}}(x, E) \equiv -\frac{d\theta}{dt} = \omega_0 \left[ 1 - \frac{x \Delta F(x)}{2E - \Delta U(x)} \right], \quad (3)$$

where  $\Delta F = -\partial_x \Delta U$ .

In order to follow the phase space evolution over many oscillation periods we consider the oscillation frequency  $\omega_{\text{osc}}(E) \equiv 2\pi/T_{\text{osc}}(E)$ , where  $T_{\text{osc}}(E) = \int_0^{2\pi} d\theta / \omega_{\text{ps}}(\theta, E)$  is the period of the motion. The deviation of this period from the harmonic period  $2\pi/\omega_0$  has the form

$$\delta T_{\text{osc}}(E) = \frac{1}{\omega_0} \int_0^{2\pi} d\theta \frac{x \Delta F/2}{E - \Delta U(x) - x \Delta F(x)/2}. \quad (4)$$

Equation (4) is exact whenever the denominator inside the integral is positive, such that the phase space trajectory of energy  $E$  completes a full round trip about the origin  $x = p = 0$ . In the weak corrugation limit we consider only the leading term and approximate the trajectories as circular with  $r = x_{\text{max}}$ , where  $x_{\text{max}}(E) = \sqrt{2E/m\omega_0^2}$  is the distance of the two harmonic turning points from the center. In this approximation we obtain

$$\delta T_{\text{osc}}(E) \approx \frac{1}{\omega_0 E} \int_{-x_{\text{max}}}^{x_{\text{max}}} \frac{x \Delta F(x) dx}{\sqrt{x_{\text{max}}^2 - x^2}}. \quad (5)$$

Equation (5) implies that the potential corrugation contributes to changes in the oscillation frequency primarily near the turning points. If the force  $\Delta F(x)$  near the turning points is directed outwards [ $x \Delta F(x) > 0$ ] then the contribution to the period  $\delta T_{\text{osc}}$  is positive and the contribution to the frequency  $\delta\omega = \omega_{\text{osc}} - \omega_0$  is negative, since it causes the atom to be delayed near the turning point. In the opposite case [ $x \Delta F(x) < 0$ ] the force repels the atom from the turning point back to the center so that the delay near the turning point is shorter and the oscillation frequency increases so that  $\delta\omega$  is positive. The angular velocity dispersion  $\delta\omega(E)$  determines the angular spread of the phase space distribution after a given evolution time.

## EXPERIMENT AND SIMULATION

We implement the experiment in an atom chip setup [26, 27], shown schematically in Fig. 1. About  $5 \times 10^7$   $^{87}\text{Rb}$  atoms are collected by a magneto-optical trap in an ultrahigh vacuum chamber. After molasses cooling we load the atomic cloud into a magnetic trap which, after RF evaporative cooling to  $\approx 400$  nK, has about 3000 atoms located  $370 \mu\text{m}$  from the chip surface. Next, we adiabatically bring the atoms to  $20 \mu\text{m}$  below the chip. A high  $x$ -axis bias field of 18 G ensures that the trap is almost perfectly harmonic in the longitudinal ( $\hat{x}$ ) direction. It is also very smooth, since the atoms are relatively far from the main trapping wire (labelled ‘‘Cu’’ in Fig. 1). These transitions further reduce the cloud temperature to 160 nK; trap frequencies are  $\omega_0 = 2\pi \times 38$  Hz (longitudinal) and about  $2\pi \times 110$  Hz (transverse), and the elastic collision rate is  $\approx 2 \text{ s}^{-1}$ . In addition, currents passing in opposite directions through the displacement wires (‘‘U’’) shift the trap center along the  $x$  axis. Suddenly turning off these wires at the beginning of our experiments then induces oscillations of the atomic cloud along the  $x$  axis of the trap at a well-defined initial time.

Different experiments are conducted with and without a small current in the corrugation wire (‘‘Z’’); when it is turned on, the distance of the atom cloud from the chip is maintained at  $20 \mu\text{m}$  by slightly reducing the current in the main trapping wire. The fabrication of the corrugation wire introduced slight mismatches at the edge of the field of view of the lithography process ( $160 \mu\text{m}$

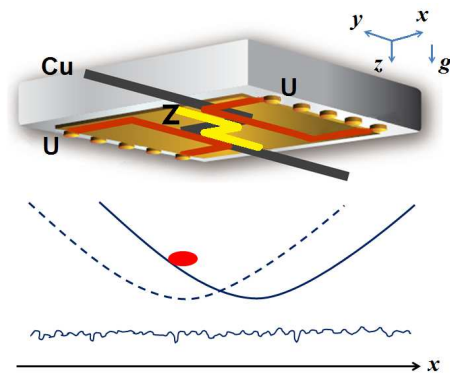


FIG. 1. (Color online) (upper) The atom chip (gold surface) acts as a mirror for the magneto-optical trap and for imaging the atomic cloud. Three wires are used to generate the potentials used in this experiment. (lower) The main trapping field is a smooth harmonic potential (dashed curve) generated by the copper Z-shaped confining wire (Cu) whose center is  $\approx 1.2$  mm above the atomic cloud; the harmonic potential is displaced (solid curve) along the  $x$  axis by currents through a pair of gold U-shaped wires (U) located  $320 \mu\text{m}$  above the atoms; the weak corrugation potential (wavy line), highly exaggerated compared to the harmonic potentials, is imposed by a small current through the atom chip Z-shaped wire (Z) located  $20 \mu\text{m}$  above the atoms. External coils creating bias fields along the  $x$  and  $y$  axes are not shown.

long). These are responsible for the largest corrugations seen in our experiments, all of which are conducted for distances  $\geq 20 \mu\text{m}$  [28].

In order to observe the phase space distribution after an oscillation time  $t_1$ , we adiabatically turn off the current in the corrugation wire and let the atoms evolve in the perfect harmonic potential for a variable time  $t_2$ . This is equivalent to performing a phase space rotation  $x \rightarrow x \cos \theta - (p/m\omega_0) \sin \theta$  and  $p \rightarrow p \cos \theta + m\omega_0 x \sin \theta$ , where  $\theta = -\omega_0 t_2$ . We then take an *in situ* absorption image of the atomic density and integrate it along the transverse direction to obtain the longitudinal density  $n(x)$ . The normalized density is equivalent to a projection of the phase space distribution  $P(\bar{q}, \bar{p})$ , where  $\bar{q} = x$  and  $\bar{p} = p/m\omega_0$  over the angle  $\theta$

$$\text{pr}(\bar{q}, \theta) = \int_{-\infty}^{\infty} d\bar{p} P(\bar{q} \cos \theta - \bar{p} \sin \theta, \bar{q} \sin \theta + \bar{p} \cos \theta). \quad (6)$$

The tomography algorithm allows the reconstruction of the original phase space distribution  $P(\bar{q}, \bar{p})$  from a series of projections at  $0 < \theta < \pi$ . The accurate form of the mathematical transformation [23]

$$P(\bar{q}, \bar{p}) = \frac{1}{2\pi^2} \int_0^\pi d\theta \int_{-\infty}^{\infty} dx K(\bar{q} \cos \theta + \bar{p} \sin \theta - x) \text{pr}(x, \theta), \quad (7)$$

with the kernel function  $K(x) = \int_0^\infty dk k \exp(ikx)$ , is replaced by a sum over a finite number of projections and an approximate non-divergent form of the kernel

$$K(x) = \begin{cases} \frac{1}{x^2} [\cos k_c x + k_c x \sin k_c x - 1] & k_c x > 0.1 \\ \frac{k_c^2}{2} \left[ 1 - \frac{k_c^2 x^2}{4} + \frac{k_c^4 x^4}{72} \right] & k_c x \leq 0.1 \end{cases} \quad (8)$$

where  $k_c$  corresponds to a wavelength on the order of the phase space resolution allowed by this algorithm ( $k_c = 0.43 \mu\text{m}^{-1}$  in our case). In our experiment we measure the atomic density at  $t_2$  time intervals of 1 ms spanning a half-period of the oscillation, giving rise to 13 images that correspond to a series of angles separated by  $\pi/13$ . To improve the signal-to-noise ratio we average 10 measurements for each angle.

We note that our tomography technique allows a full reconstruction of the phase space distribution. A previous tomographic reconstruction used a free space propagation method for changing the projection angle [25, 29], valid only for the restricted range 0 to  $\pi/2$ , while the rest of the angles were obtained by a symmetry assumption. In contrast, our method spans the full range of  $\theta$  from 0 to  $\pi$ , thereby implementing one of the procedures suggested in Ref. [30].

In the first series of experiments (Fig. 2), we force the cloud to oscillate with an amplitude of  $85 \mu\text{m}$ . When there is no current in the corrugation wire, the phase space distribution maintains an approximately isotropic Gaussian shape, even after oscillating for 500 ms, as

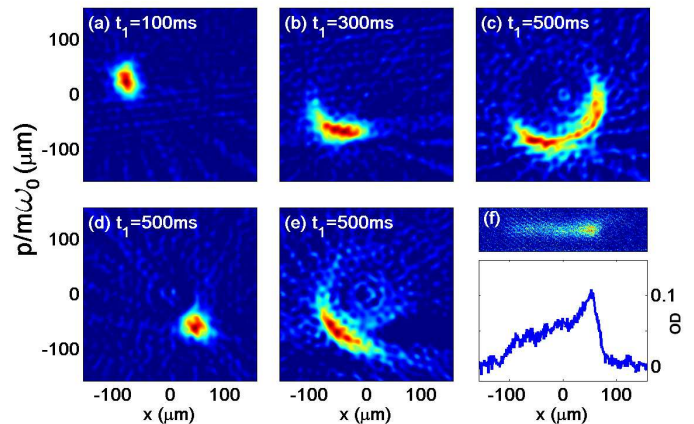


FIG. 2. (Color online) Reconstructed phase space distributions (a-c) with a 5 mA current in the corrugation wire, an  $85 \mu\text{m}$  oscillation amplitude, and oscillation times  $t_1$  as shown. The distribution in (d) is obtained with the corrugation wire turned off, while that shown in (e) is obtained by translating the equilibrium position of the cloud by  $73 \mu\text{m}$  using the displacement wires. (f) A typical *in situ* image and its corresponding one-dimensional density distribution, selected from the data set used for reconstructing the  $t_1 = 500$  ms phase space distribution shown in (c).

shown in Fig. 2(d). This demonstrates that the trap potential is almost purely harmonic. Applying a 5 mA current to the corrugation wire gives rise to dramatic changes. After an oscillation time of 100 ms, the phase space distribution develops a slight deformation, which appears more distinctly after 300 ms, as shown in Fig. 2(a-b). After oscillating for 500 ms, the phase space distribution develops a crescent-shaped pattern totally unlike that for the purely harmonic potential, as shown in Fig. 2(c).

We conducted a second experiment to examine the effect produced by a different region along the corrugation potential by displacing the equilibrium position along the longitudinal axis and forcing oscillations with a slightly shorter amplitude ( $80 \mu\text{m}$ ). Differences between the resulting phase space distribution [Fig. 2(e)] and that shown in Fig. 2(c) may therefore be attributed to differences of the corrugation potential in their respective oscillation ranges, the reasons for which are discussed further below.

The phase-space dynamics of this system can be accurately simulated if the potential is known. The potential corrugation  $\Delta U(x)$  was extracted from a series of measurements of the equilibrium density  $n(x)$  of the atomic cloud in the presence of a harmonic potential [15] centered  $20 \mu\text{m}$  below multiple positions along the corrugation wire, as shown in Fig. 3. In order to observe atom density modulations due to random current fluctuations more clearly, we increased the corrugation-wire current to 40 mA, an 8-fold increase over that used for our oscil-

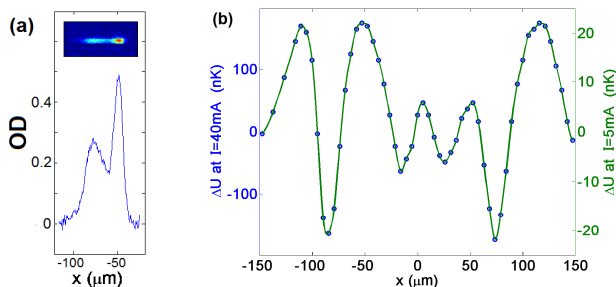


FIG. 3. (Color online) Measurements of the corrugation potential at a height of  $20 \mu\text{m}$  for a current of  $40 \text{ mA}$ . (a) Typical image of the atomic cloud optical density (OD) distribution for one particular current in the displacement wires. (b) The potential along the entire length of the corrugation wire, as reconstructed from a series of measurements like those in (a) that overlap along the  $x$  axis. The right-hand scale shows the potential corresponding to the corrugation wire current of  $5 \text{ mA}$  used in the oscillation experiments.

lation experiments. The current through the main trapping wire was correspondingly reduced to maintain the atom cloud at a distance of  $20 \mu\text{m}$  from the corrugation wire.

At  $5 \text{ mA}$ , the main feature of the corrugation potential are two wells with amplitudes of  $\pm 22 \text{ nK}$  centered at  $x \approx \pm 80 \mu\text{m}$  caused, as noted, by mismatches at the edges of the field of view of the lithography process. In between lie two additional shallower wells of amplitude  $\pm 7 \text{ nK}$ . In our first experiment [Fig. 2(a-c)] the two classical turning points of the oscillation lie near the two deepest wells. This implies a force in the outward direction [ $x\Delta F(x) > 0$ ] for lower energies, giving rise to a longer oscillation period [ $\delta T_{\text{osc}} > 0$  in Eq. (5)] and hence smaller oscillation frequency ( $\delta\omega < 0$ ), while higher energies correspond to a force directed inward [ $x\Delta F(x) < 0$ ], and hence a higher oscillation frequency ( $\delta\omega > 0$ ). Conversely, the two turning points are located at  $x \approx 0$  and  $x \approx 160 \mu\text{m}$  in our second experiment, where the potential wells are much shallower. Qualitatively, this should give rise to a smaller phase space angular dispersion, as shown by Fig. 2(e).

For a more quantitative comparison, we begin with Eq. (4) and calculate the oscillation frequency for any given particle energy, as shown in Fig. 4. Preparing a random Boltzmann distribution of atoms in a trap shifted by  $x_{\text{shift}} = 85 \mu\text{m}$  and then releasing it suddenly to the original position, as performed in the experiments, produces an energy distribution centered at  $E_{\text{shift}} = \frac{1}{2}m\omega_0^2 x_{\text{shift}}^2$  and having a standard deviation  $\Delta E \approx \sqrt{k_B T(k_B T + 2E_{\text{shift}})}$ . This energy distribution (shown in Fig. 4) involves phase space trajectories with frequency shifts between  $\delta\omega/\omega_0 \approx -0.015$  at  $E \sim 0.73 E_{\text{shift}}$  and  $\delta\omega/\omega_0 \approx +0.009$  at  $E \sim 1.2 E_{\text{shift}}$  (red dots in Fig. 4). It follows that the angular dispersion after time  $t_1$  is  $\Delta\theta \sim 0.024\omega_0 t_1 \approx 2.85$  radians, as in-

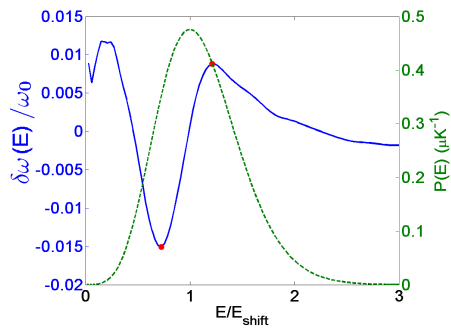


FIG. 4. (Color online) (solid curve) Frequency shift  $\delta\omega$  as a function of the longitudinal energy of an atom in a harmonic trap centered at  $x = 0$  in the presence of the corrugation potential [Fig. 3(b)]. The energy is in units of  $E_{\text{shift}} = \frac{1}{2}m\omega_0^2 x_{\text{shift}}^2$ , where  $x_{\text{shift}} = 85 \mu\text{m}$  is the position of the initial trap center used for preparing the atoms. (dashed curve) Energy distribution for an atomic ensemble prepared in the initial trap centered at  $x_{\text{shift}}$ . The ensemble contains atoms whose energies span reduced oscillation frequencies (near  $E = 0.73 E_{\text{shift}}$ ) to increased oscillation frequencies (near  $E = 1.23 E_{\text{shift}}$ ) (red dots). The evolution that follows leads to the simulated phase space distributions shown in Fig. 5(a).

deed observed in the experimental phase space distribution [Fig. 2(c)].

In Fig. 5(a) we show the results of a simulation based on adding a proper phase space angle to each atom in the random distribution according to  $\delta\omega(E)$  in Fig. 4. For comparison, Fig. 5(b) shows the phase space distribution resulting from a full calculation based on a direct numerical solution of the equations of motion [Eq. (1)] in the presence of the corrugation potential. In addition, we account for collisions by assuming that the probability of collision between each pair of atoms in a small volume  $V$  during a time interval  $\tau$  is  $\sigma_{\text{el}} v_{\text{rel}} \tau / V$ , where  $\sigma_{\text{el}} = 8 \cdot 10^{-12} \text{ cm}^2$  is the  $s$ -wave collision cross-section and  $v_{\text{rel}}$  is the relative velocity between the two atoms. This implies that higher collision probabilities are expected between pairs of atoms which occupy the same volume but have opposite velocity. Such events become more probable when the phase space angular distribution becomes more dispersed. When a collision occurs, the two atoms scatter into new velocities along the  $x$  direction and the center of mass velocity is conserved, while the energy is redistributed between the longitudinal and transverse degrees of freedom.

For generating Fig. 5(b) we also simulated the effect of finite imaging resolution and repeated the tomography procedure. The result is very similar to the collisionless phase-space dispersion calculation in Fig. 5(a). The main features of the phase space distribution are similar to those observed in the experiment. The rather small differences may stem from effects that were not taken into account, such as coupling between the longitudinal and

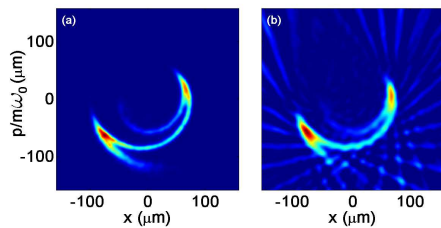


FIG. 5. (Color online) Phase space distribution obtained by simulation. (a) The simulation was based on preparing an ensemble of atoms with a thermal distribution in the initial trap and then adding a proper phase space angle according to  $\delta\omega(E)$  in Fig. 4. (b) The full equations of motion [Eq. (1)] were numerically solved for each atom and collisions were also included. We also repeated the tomography algorithm and took into account the finite resolution of the optical system. The similarity between (a) and (b) shows that for a collision rate of about  $2\text{s}^{-1}$  there is no significant smearing of the phase space distribution, even after 500 ms. The main features observed in the experiment [Fig. 2(c)] are predicted by these simulations.

transverse degrees of freedom by potential distortions of a three-dimensional nature and additional shot-to-shot noise in the experiment.

## DISCUSSION AND CONCLUSION

To conclude, we have studied the classical phase space evolution of trapped atoms oscillating in a harmonic potential with static corrugations along one dimension. For oscillation times on the order of the mean time between collisions, phase space variables propagate along nearly circular iso-energetic trajectories whose angular velocity dispersion is determined mainly by potential corrugations near the classical turning points. We observe squeezing of the phase space distribution, the deformation of which is very sensitive to fine details of the potential corrugations.

As long as collisions are rare and dimensions are separable, the phase space area is conserved during the squeezing effect, and lower densities and temperatures of the atomic ensemble can be reached, as in delta-kick cooling [31]. Comparison of our experiment with a simulation that takes collisions into account suggests that the collisionless phase space features are not drastically smeared in the presence of a small number of collisions (up to one collision per atom). The observed phase space smearing may stem from slight non-separability of the real three-dimensional potential.

We have demonstrated a novel phase space tomography method, which can serve as a tool for probing classical dynamics of trapped atoms. By using this method we were able to measure the main features of weak potential corrugations having an rms amplitude of  $\sim 10\text{nK}$ . In view of Eq. (5), the sensitivity to potential corrugations

may be improved by reducing the oscillation frequency and maintaining its amplitude. Further improvements of about one order of magnitude may be achieved by probing a longer time evolution of cold fermions or a one-dimensional ultracold Bose gas [32, 33], where the effects of collisions are suppressed. If the phase space distribution is generalized to a Wigner function [23, 34], the method could also be applied to quantum dynamics [30].

Probing, understanding, and controlling the phase space evolution of cold atoms in the presence of a corrugated potential may be important, for example, in future schemes of guided matter-wave interferometry [16, 17] and free-oscillation atom interferometry [18]. Such schemes involve splitting atomic wavefunctions into a superposition of spatially separated paths and then combining them to form an overlap in position and momentum. Measurement of the classical phase space evolution along the separated paths will enhance our understanding of the effects of potential corrugations on this kind of interferometry.

We are grateful to the members of the atom chip group and especially to Shimon Machluf for helpful discussions and to Zina Binshtok, Yaniv Bar-Haim, Benny Hadad, and Jurgen Jopp for technical support. This work was supported by the Israeli Science Foundation and by the FP7 European consortium “matter-wave interferometry” (601180). We also acknowledge support from the PBC program for outstanding postdoctoral researchers of the Israeli Council for Higher Education.

---

\* Present address: Observatoire de la Côte d’Azur, Université de Nice-Sophia Antipolis, CNRS, Parc Valrose, F-06108 Nice Cedex 2, France.

† Present address: Physics Department, Nuclear Research Center Negev, Beer-Sheva 84109, Israel.

‡ Corresponding author; [mkeil@netvision.net.il](mailto:mkeil@netvision.net.il)

- [1] P. W. Anderson. Absence of Diffusion in Certain Random Lattices. *Phys. Rev.*, 109:1492, 1958. doi=10.1103/PhysRev.109.1492. (cited on page 1).
- [2] J. Billy, V. Josse, Z. Zuo, A. Bernard, B. Hambrecht, P. Lugan, D. Clément, L. Sanchez-Palencia, P. Bouyer, and A. Aspect. Direct observation of Anderson localization of matter waves in a controlled disorder. *Nature*, 453:891, 2008. doi=10.1038/nature07000.
- [3] J. Chabé, G. Lemarié, B. Grémaud, D. Delande, P. Szriftgiser, and J. C. Garreau. Experimental Observation of the Anderson Metal-Insulator Transition with Atomic Matter Waves. *Phys. Rev. Lett.*, 101:255702, 2008. doi=10.1103/PhysRevLett.101.255702. (cited on page 1).
- [4] J. Masoliver and A. Ros. Integrability and chaos: the classical uncertainty. *Eur.J.Phys.*, 32:431, 2011. doi:10.1088/0143-0807/32/2/016. (cited on page 1).
- [5] Y. Braiman, J. F. Lindner, and W. L. Ditto. Taming spatiotemporal chaos with disorder. *Nature*, 378:465, 1995. doi=10.1038/378465a0. (cited on page 1).

- [6] N. V. Alexeeva, I. V. Barashenkov, and G. P. Tsironis. Impurity-Induced Stabilization of Solitons in Arrays of Parametrically Driven Nonlinear Oscillators. *Phys. Rev. Lett.*, 84:3053, 2000. doi=10.1103/PhysRevLett.84.3053. (cited on page 1).
- [7] T. Wulf, B. Liebchen, and P. Schmelcher. Disorder Induced Regular Dynamics in Oscillating Lattices. *Phys. Rev. Lett.*, 112:034101, 2014. doi=10.1103/PhysRevLett.112.034101. (cited on page 1).
- [8] J. Fortágh and C. Zimmermann. Magnetic microtraps for ultracold atoms. *Rev. Mod. Phys.*, 79:235, 2007. doi=10.1103/RevModPhys.79.235. (cited on page 1).
- [9] D.-W. Wang, M. D. Lukin, and E. Demler. Disordered Bose-Einstein Condensates in Quasi-One-Dimensional Magnetic Microtraps. *Phys. Rev. Lett.*, 92:076802, 2004. doi=10.1103/PhysRevLett.92.076802. (cited on page 1).
- [10] S. Aigner, L. Della Pietra, Y. Japha, O. Entin-Wohlman, T. David, R. Salem, R. Folman, and J. Schmiedmayer. Long-Range Order in Electronic Transport Through Disordered Metal Films. *Science*, 319:1226, 2008. doi=10.1126/science.1152458. (cited on page 1).
- [11] Y. Japha, O. Entin-Wohlman, T. David, R. Salem, S. Aigner, J. Schmiedmayer, and R. Folman. Model for Organized Current Patterns in Disordered Conductors. *Phys. Rev. B*, 77:201407(R), 2008. doi=10.1103/PhysRevB.77.201407. (cited on page 1, 6).
- [12] R. Folman, P. Treutlein, and J. Schmiedmayer. Atom Chip Fabrication. In J. Reichel and V. Vuletić, editors, *Atom Chips*, chapter 3, page 61. Wiley-VCH, Weinheim, Germany, 2011. doi=10.1002/9783527633357.ch3. (cited on page 1).
- [13] J. Reichel. Trapping and Manipulating Atoms on Chips. In J. Reichel and V. Vuletić, editors, *Atom Chips*, chapter 2, page 33. Wiley-VCH, Weinheim, Germany, 2011. doi=10.1002/9783527633357.ch2. (cited on page 1).
- [14] S. Kraft, A. Günther, H. Ott, D. Wharam, C. Zimmermann, and J. Fortágh. Anomalous longitudinal magnetic field near the surface of copper conductors. *J. Phys. B*, 35:L469, 2002. doi=10.1088/0953-4075/35/21/102. (cited on page 1).
- [15] J.-B. Trebbia, C. L. Garrido Alzar, R. Cornelussen, C. I. Westbrook, and I. Bouchoule. Roughness Suppression via Rapid Current Modulation on an Atom Chip. *Phys. Rev. Lett.*, 98:263201, 2007. doi=10.1103/PhysRevLett.98.263201. (cited on page 1, 3).
- [16] Y. Avishai Y. Japha, O. Arzouan and R. Folman. Using Time-Reversal Symmetry for Sensitive Incoherent Matter-Wave Sagnac Interferometry. *Phys. Rev. Lett.*, 99:060402, 2007. doi=10.1103/PhysRevLett.99.060402. (cited on page 1, 5).
- [17] S. Wu, E. Su, and M. Prentiss. Demonstration of an Area-Enclosing Guided-Atom Interferometer for Rotation Sensing. *Phys. Rev. Lett.*, 99:173201, 2007. doi=10.1103/PhysRevLett.99.173201. (cited on page 1, 5).
- [18] R. H. Leonard and C. A. Sackett. Effect of trap anharmonicity on a free-oscillation atom interferometer. *Phys. Rev. A*, 86:043613, 2012. doi=10.1103/PhysRevA.86.043613. (cited on page 1, 5).
- [19] Y. Japha and Y. B. Band. Motion of a condensate in a shaken and vibrating harmonic trap. *J. Phys. B*, 35:2383, 2002. doi=10.1088/0953-4075/35/10/315. (cited on page 1).
- [20] D. D. Nolte. The tangled tale of phase space. *Phys. Today*, 63:33, 2010. doi=10.1063/1.3397041. (cited on page 1).
- [21] A. Bertoldi and L. Ricci. Dynamics of a cold atom cloud in an anharmonic trap. *Phys. Rev. A*, 81:063415, 2010. doi=10.1103/PhysRevA.81.063415. (cited on page 1).
- [22] I. Llorente García, B. Darquié, C. D. J. Sinclair, E. A. Curtis, M. Tachikawa, J. J. Hudson, and E. A. Hinds. Shaking-induced dynamics of cold atoms in magnetic traps. *Phys. Rev. A*, 88:043406, 2013. doi=10.1103/PhysRevA.88.043406. (cited on page 1).
- [23] U. Leonhardt. *Measuring the quantum state of light*. Cambridge University Press, New York, 2005. ISBN=978-0-521-02352-8. (cited on page 1, 3, 5).
- [24] A. I. Lvovsky, H. Hansen, T. Aichele, O. Benson, J. Mlynek, and S. Schiller. Quantum State Reconstruction of the Single-Photon Fock State. *Phys. Rev. Lett.*, 87:050402, 2001. doi=10.1103/PhysRevLett.87.050402. (cited on page 1).
- [25] Ch. Kurtsiefer, T. Pfau, and J. Mlynek. Measurement of the Wigner function of an ensemble of helium atoms. *Nature*, 386:150, 1997. doi=10.1038/386150a0. (cited on page 1, 3).
- [26] R. Folman, P. Krüger, J. Schmiedmayer, J. Denschlag, and C. Henkel. Microscopic atom optics: from wires to an atom chip. *Adv. At. Mol. Opt. Phys.*, 48:263, 2002. doi=10.1016/S1049-250X(02)80011-8. (cited on page 2).
- [27] J. Reichel. Microchip traps and Bose-Einstein condensation. *Appl. Phys. B*, 74:469, 2002. doi=10.1007/s003400200861. (cited on page 2).
- [28] For a different experiment, the edges of the corrugation wire are modulated with a period of  $5\ \mu\text{m}$ , giving rise to a short-range sinusoidal potential. As demonstrated in previous work [11] however, the magnetic field at  $20\ \mu\text{m}$  distance is not influenced by the  $5\ \mu\text{m}$  periodic edge modulation and variations of the magnetic field are dominated by imperfections in the wire edge over a longer scale. Explicit numerical simulations of the magnetic potential confirm that residual sinusoidal corrugation (due to the  $5\ \mu\text{m}$ -period modulation of the corrugation wire edges) is  $\ll 1\ \text{nK}$  and is therefore negligible under the conditions of these experiments. (cited on page 3).
- [29] T. Pfau and Ch. Kurtsiefer. Partial reconstruction of the motional Wigner function of an ensemble of helium atoms. *J. Mod. Optic.*, 44:2551, 1997. doi=10.1080/09500349708231900. (cited on page 3).
- [30] A. del Campo, V. I. Manko, and G. Marmo. Symplectic tomography of ultracold gases in tight waveguides. *Phys. Rev. A*, 78:025602, 2008. doi=10.1103/PhysRevA.78.025602. (cited on page 3, 5).
- [31] H. Ammann and N. Christensen. Delta Kick Cooling: A New Method for Cooling Atoms. *Phys. Rev. Lett.*, 78:2088, 1997. doi=10.1103/PhysRevLett.78.2088. (cited on page 5).
- [32] T. Kinoshita, T. Wenger, and D. S. Weiss. A quantum Newtons cradle. *Nature*, 440:900, 2006. doi=10.1038/nature04693. (cited on page 5).
- [33] I. E. Mazets and J. Schmiedmayer. Thermalization in a quasi-one-dimensional ultracold bosonic gas. *New J. Phys.*, 12:055023, 2010. doi=10.1088/1367-2630/12/5/055023. (cited on page 5).
- [34] C.-Y. Wong. Explicit solution of the time evolution of the Wigner function. *J. Opt. B*, 5:S420, 2003. doi=10.1088/1464-4266/5/3/381. (cited on page 5).